SCIENCE CHINA Materials ARTICLES

mater.scichina.com link.springer.com

Published online 26 October 2017 | https://doi.org/10.1007/s40843-017-9127-0

Sci China Mater 2018, 61(3): 401–408

Au NP@silica@europium coordination polymer nanocomposites for enhanced fluorescence and more sensitive monitoring reactive oxygen species

Huiqin Li[1*], Jianhui Yang[2*], Qingqing Deng[2], Shumei Dou[1], Weiwei Zhao[1], Chong Lin[2] and Xiaofang Liu[2]

ABSTRACT **Au nanoparticle (Au NP)@SiO_2@TDA-Eu nanocomposites were prepared by a two-step process: Au NP@SiO_2 nanocomposites were prepared by a modified one-pot process. Then the europium coordination polymer was deposited on the surface of the Au NP@SiO_2 by mixing 2,2′-thiodiacetic acid [$S(CH_2COO)_2^{2-}$, TDA] and $Eu(NO_3)_3{\cdot}6H_2O$ in ethanol *via* a hydrothermal method. The maximum fluorescent enhancement factor of the nanocomposites was 6.81 at 30 nm thickness of silica between the core of the Au NP and the shell of TDA-Eu. The prepared nanocomposites exhibit more sensitive monitoring of reactive oxygen species.**

Keywords: nanocomposites, fluorescence enhancement, silica, coordination polymers, reactive oxygen species

INTRODUCTION

Reactive oxygen species (ROS, such as $O_2^{\bullet-}$, RO·, H_2O_2, $^1O_2$, etc.) have been considered to play important roles in human mortality and morbidity [1,2]. Fluorescence detection has been considered to be the most powerful technique due to its high sensitivity and experimental convenience. Rare earth ion (especially trivalent lanthanide ions of Eu) luminescence is attracting considerable attention due to their outstanding optical properties and growing applications in optical devices and biomedical fields such as therapeutic and imaging probes [3–6]. Compared to trivalent lanthanide ions doped with oxidative species and rare earth complexes, a new type of organic-inorganic hybrid materials of rare-earth coordination polymers (CPs) or lanthanide-organic frameworks is showing promising because of the intrinsic properties of the trivalent lanthanide ions and the electrostatic nature of the coordination chemistry, which allow a large variety of symmetries and structural patterns to be obtained [7,8]. However, low fluorescent efficiency still exists and hinders the development of lanthanide-organic frameworks. Therefore, increasing the fluorescent emission intensities of lanthanide-organic frameworks is critical to realization of their use in sensors.

Regarding this, Au@SiO_2 core-shell nanoparticles (NPs) are of great interest due to metal-enhanced fluorescent effects based on the surface plasmon resonance (SPR) of Au NPs [9–14]. Fluorescence quenching also occurs by non-radiation energy transfer if the chromophore is situated in vicinity of Au NPs. The enhancing and quenching effects strongly depend on the distance between the surface of Au NPs and chromophores [15–20]. In the present work, we prepared Au NP@silica@europium coordination polymers denoted as Au NP (Au NP)@SiO_2@TDA-Eu nanocomposites by two steps: first, Au NP@SiO_2 nanaocomposites were prepared by a modified one-pot process [21,22]. The europium coordination polymers were then deposited on the surface of Au NP@SiO_2 by mixing 2,2′-thiodiacetic acid [$S(CH_2COO)_2^{2-}$, TDA] and $Eu(NO_3)_3{\cdot}6H_2O$ in ethanol. The prepared Au NP@SiO_2@TDA-Eu samples were further used to detect ROS (H_2O_2).

EXPERIMENTAL SECTION

The fabrication of Au NP@SiO_2@TDA-Eu nanocompo-

[1] Department of Chemistry and Chemical Engineering, Baoji University of Arts and Sciences, Shaanxi Key Laboratory of phytochemistry, Baoji 721013, China

[2] Key Laboratory of Synthetic and Natural Functional Molecule Chemistry (Ministry of Education), Shaanxi Key Laboratory of Physico-Inorganic Chemistry, College of Chemistry & Materials Science, Northwest University, Xi'an 710127, China

* Corresponding authors (emails: huiqinli@yeah.net (Li H); jianhui@nwu.edu.cn (Yang J))

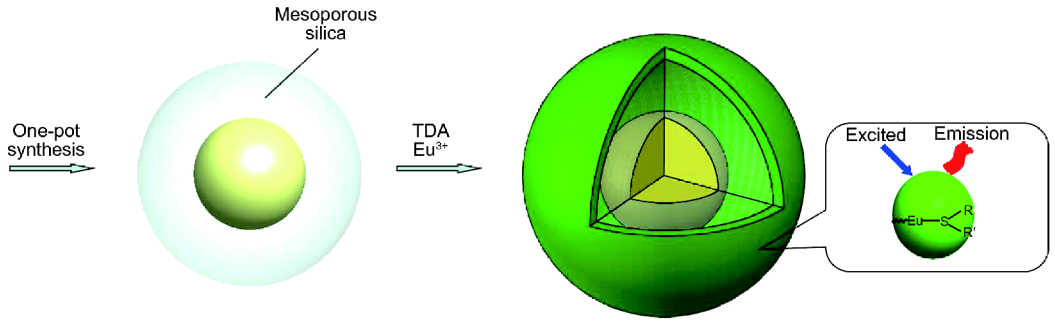

Figure 1 Schematic illustration of the Au NP@SiO_2@TDA-Eu nanocomposite.

sites are shown in Fig.1. At first, Au NP@SiO_2 core-shell nanostructures with different silica thicknesses were prepared by a one-pot process, in which the diameter of Au NP was about 10 nm, and a core-shell structure of Au NP@SiO_2 was obtained through the hydrolysis of tetraethyl orthosilicate (TEOS) under alkaline conditions. As the spacer layer, the thickness of silica could be controlled from 10 to 40 nm by changing the amount of TEOS. Subsequently, a europium coordination polymer (TDA-Eu) was then deposited on the surface of Au NP@SiO_2 nanostructures by hydrothermal treatment [23]. The resulting Au NP@SiO_2@TDA-Eu nanocomposites with core@spacer@shell structure are obtained.

Chemicals

Chloroauric acid ($HAuCl_4{\cdot}4H_2O$, 99.999%), cetyltrimethylammonium bromide (CTAB, 99.0%), sodium hydroxide (NaOH, >96%), formaldehyde solution (CH_4O, 37.0%), 2,2'-thiodiacetic acid (TDA), europium nitrate hexahydrate ($Eu(NO_3)_3{\cdot}6H_2O$), ethanol (C_2H_6O, 95.0%), and tetraethyl orthosilicate (TEOS, >98.0%) with analytical grade, were purchased from Beijing Chemical Reagents Factory and used without further purification. Deionized water was used for all experiments.

Synthesis of Au NP@SiO_2 core–shell nanocomposite

The Au NP@SiO_2 core-shell nanostructures were synthesized according to a modified one-pot process. (0.05 g) CTAB and (0.5 mol L^{-1}, 600 mL) NaOH were dissolved in 24 mL of deionized water. The solution was heated to 80°C and held for 15 min. Then, 1 mL of formaldehyde solution (37%) and 0.04 mmol of $HAuCl_4{\cdot}4H_2O$ were added and the resulting solution changed to gray over a few seconds and eventually to wine-red. After stirring for 10 min, Au NP@SiO_2 NPs were subsequently synthesized by adding a mixed liquid of TEOS and ethanol and heated in a water bath for 6 h. The spacer thickness of silica could be adjusted to about 10, 20, 30 and 40 nm by adding the amount of TEOS 500, 580, 720 and 900 μL, respectively. In this process, Au NPs were obtained by reducing chloroauric acid with formaldehyde, furthermore, using CTAB as a template, Au@SiO_2 NPs were formed through hydrolysis of TEOS under alkaline condition to deposit silica on the surface of Au [21], which needed to strictly control the reaction time at 10 min, after TEOS was added, the mixing speed should be adjusted below 400 rpm, the reaction time was so long enough to ensure that the silica could completely self-assembled. After reaction, the samples with relatively uniform size were obtained by centrifugation.

Synthesis of Au NP@SiO_2@TDA-Eu nanocomposite

The mixture of TDA (60 mg), $Eu(NO_3)_3{\cdot}6H_2O$ (80 mg) and Au NP@SiO_2 core-shell nanostructures synthesized in the previous step were dissolved in 20 mL ethanol. After being degassed using N_2 for 10 min, the mixture was put into a Teflon autoclave and heated to 100°C for 24 h. $[Eu_2(TDA)_3]{\cdot}2H_2O$ [24] was formed on the surface of Au NP@SiO_2 and the resulting product of Au NP@SiO_2@TDA-Eu nanocomposites were obtained by centrifugation. The fluorescent property of the Au NP@SiO_2@TDA-Eu nanocomposites with different thickness of silica was detected under the same concentration of Eu^{3+} in ethanol. In order to keep the concentration of Eu^{3+} consistent, the synthesis process was carried out with excessive TDA and kept long enough to allow the TDA-Eu to be completely modified on the surface of Au NP@SiO_2. The concentration of Eu^{3+} was set to 0.5 g L^{-1} which was obtained by dispersing the reaction liquid in ethanol by ultrasonication with the constant volume of 160 mL. The same amount of solution was used to measure the fluorescence data, and the average values of the three experiments were reported. In addition, in order to reflect the fluorescence enhancement

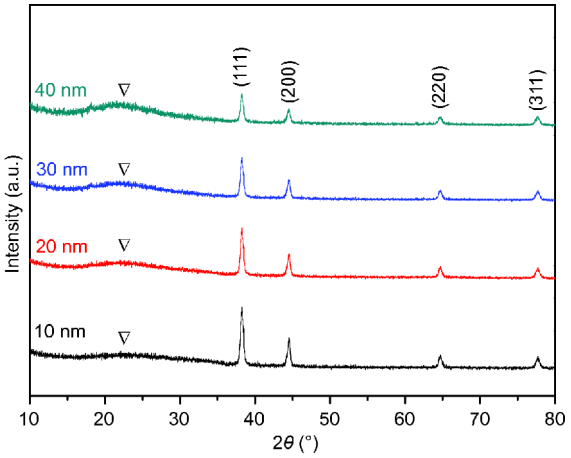

Figure 2 XRD patterns of the Au NP@SiO_2 with different silica thicknesses of 10, 20, 30 and 40 nm, respectively.

effect of Au, the samples of 'no Au spheres' were synthesised by the same process but no adding $HAuCl_4 \cdot 4H_2O$, forming the SiO_2@TDA-Eu nanocomposites.

Monitoring the fluorescence of Au NP@SiO_2@TDA-Eu after reacting with H_2O_2

The concentration of Eu^{3+} was fixed at 10 mg mL^{-1}. 0.5 mL of the TDA-Eu and Au NP@SiO_2@TDA-Eu were dispersed in ethanol solution, then were treated with (500 μL H_2O_2 with different concentrations from 0 to 500 μmol L^{-1} for 10 min, respectively. The solutions were then centrifuged at 8,000 rpm to remove excess hydrogen peroxide solution. The Au NP@ SiO_2@DTA-Eu-H_2O_2 and DTA-Eu-H_2O_2 were re-dispersed in 200 mL of anhydrous ethanol, then, 40 μL of the above solution were respectively dropped into the center of the quartz plate of 1 cm^2 and dried at 30°C. The fluorescence emissions were monitored at room temperature from 500–700 nm using a xenon lamp as the light source with an excitation wavelength of 399 nm wavelength of excitation, a 10 nm width, and 0.5 sec response time.

Characterization

Transmission electron microscopy (TEM) and high-resolution TEM analyses were carried out on a JEOL JEM-2010F transmission electron microscope equipped with a field emission gun operated at 200 kV. UV-vis absorption spectra was recorded using a TU-1901 spectrophotometer. X-ray diffraction (XRD) analysis was recorded using a Hitachi S-5500 at an accelerating voltage of 20 kV. Energy dispersive spectroscopy (EDS) was carried out by a field emission scanning electron microscopy (SEM, SIGMA ZEISS). Room-temperature fluorescence emission spectra and fluorescent decay were taken through F-4500 fluorescence spectrophotometer of Hitachi Company.

RESULTS AND DISCUSSION

The phase and composition of the Au NP@SiO_2 core-shell nanostructures prepared by one-pot process were characterized by XRD in Fig. 2. Au characteristic peaks could easily be assigned to the (111), (200), (220), and (311) planes of a cubic face-centered phase (JCPDS card PDF#04-0784). And there is a broad peak between 20 and 25 marked with hollow triangles which is assigned to the silica (JCPDS card PDF#38-0651) shell [24]. The diffraction peak intensity of Au decreased with increasing the silica thickness. The Au NP@SiO_2 core-shell nanostructure was further characterized with TEM.

Au NPs with a diameter of 10 nm are displayed in Fig. 3a and high resolution TEM is shown in the inset of Fig. 3a with the crystal plane spacing being 0.24 nm, which is corresponds to the Au (111) plane. The typical Au NP@SiO_2 core-shell nanostructures with different silica thickness of 10–40 nm are shown in Fig. 3b–e. The thickness of the silica was controlled by TEOS concentration in the mixtures of ethanol where the volumes of the added TEOS were 500, 580, 720 and 900 μL, respectively. After depositing TDA-Eu onto the outer surface of the Au NP@SiO_2 core-shell nanostructure, the core-layer-shell structure of Au NP@SiO_2@TDA-Eu was shown in Fig. 3f, furthermore, the Eu, Si, S, C and O signals can be observed in the EDS plot given in the inset of Fig. 3f.

Fig. 4a shows the absorption spectra of aqueous dispersions of pure TDA and Au NP@SiO_2@TDA-Eu nanocomposites. There is an absorption peak at 236 nm for the pure DTA, while the absorption peak disappears when Eu coordinates with DTA, which is due to the interaction between inorganic Eu^{3+} and the free electrons on the –COOH of TDA, inducing significant alteration of the polarity of the coordination environment of Eu^{3+}. The other obvious absorption peak of Au NP@SiO_2@TDA-Eu nanocomposites appears at 540 nm signed with a diamond, which belongs to the surface plasmon resonance of Au NPs. As shown in Fig. 4b, the absorption peaks of the nanocomposites are red-shifted from 528 to 545 nm as the silica thickness increased from 10 to 40 nm. Because of the surface plasmon resonances related to the dielectric constant of the metal and surrounding dielectric, the wavelength will be red-shift after coating silica shell with refractive index (n =1.4585) compared with water (n =

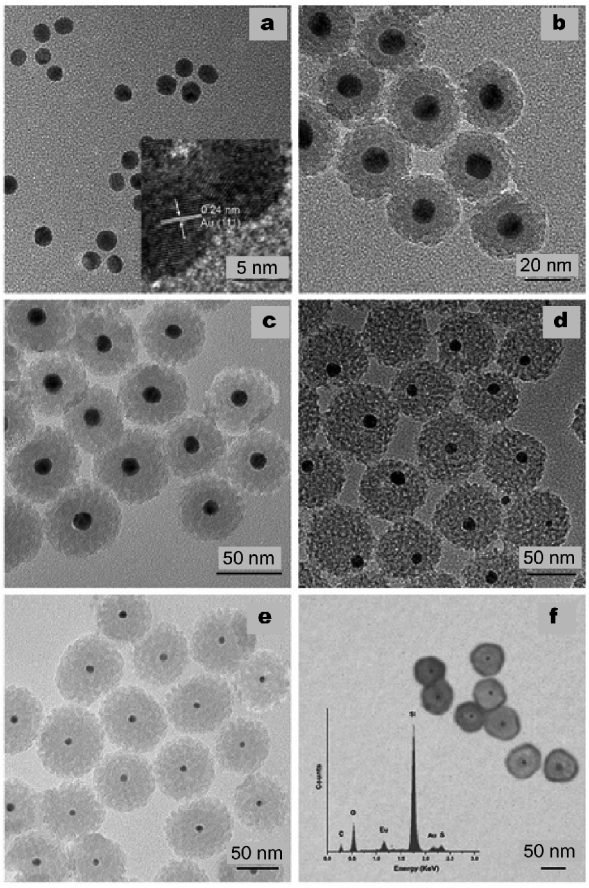

Figure 3 TEM (a) and high-resolution images of Au NPs, TEM images of Au NP@SiO_2 core-shell nanostructures with different silica thickness of (b) 10 nm, (c) 20 nm, (d) 30 nm and (e) 40 nm, TEM (f) Au NP@SiO_2@TDA-Eu nanocomposite and its electronic energy spectrum, respectively.

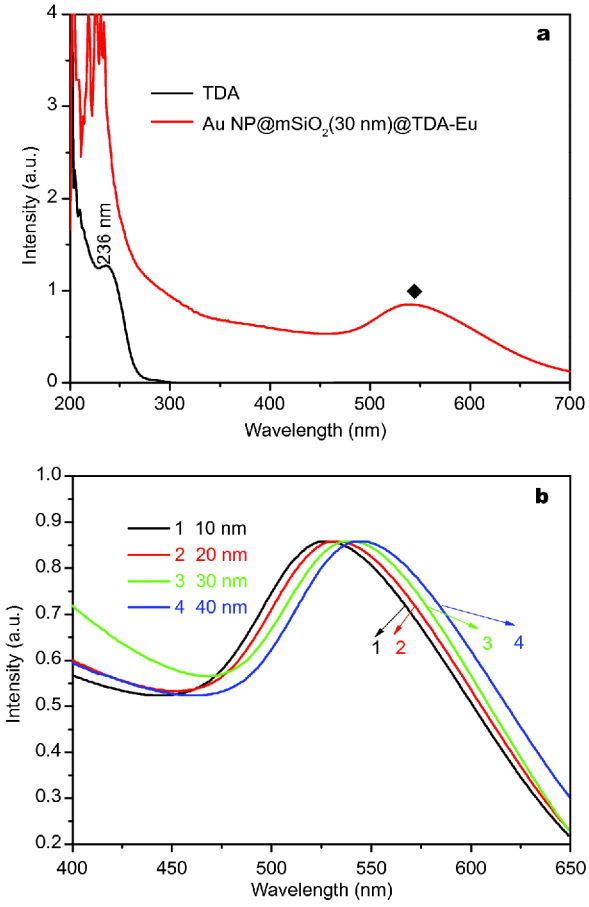

Figure 4 (a) UV-vis spectra of pure TDA and Au NP@SiO_2@TDA-Eu nanocomposites, (b) Au NP@SiO_2@TDA-Eu nanocomposites with different silica thickness.

1.3325) [25,26]. And also the redshift is obviously dependent on the thickness of silica shell.

The excitation and emission spectra of Au NP@SiO_2@TDA-Eu in ethanol are shown in Fig. 5. The maximum emission peak at 399 nm was obtained at a excitation wavelength of 616 nm in Fig. 5a, and the emission spectrum displays two clear peaks in Fig. 5b at 594 and 619 nm, which correspond to the transition of the Eu^{3+} excited states $^5D_0 \rightarrow {}^7F_1$ and $^5D_0 \rightarrow {}^7F_2$, respectively [27–29].

As shown in Fig. 6a, the fluorescence emission spectra are obtained using a 399 nm excitation wavelength at room temperature. It can be seen that the intensity of fluorescence emission increases and then reduces with increasing thicknesses of the silica layer. When the thickness of silica layer is about 30 nm, the fluorescence emission intensity of the nanocomposites is the strongest. The average maximum enhancement factor is 6.81. The maximum value of fluorescence intensity appears around 30 nm of silica layer thickness.

Based on the theoretical model of local electromagnetic field and radioactive decay lifetimes, it is considered that the excitation of surface plasmons will induce the enhancement of the local electromagnetic field. These enhanced regions can also change the local electromagnetic field density [29], and the enhancement of fluorescence emission depends on the competition of the distance-dependent mechanism [17,30]. However, at the same time, it will also create faster radiation decays [31–33]. In order to verify the relationship between fluorescence enhancement and lifetime decay, the fluorescence lifetime is tested as shown in Fig. 7, where the fluorescence lifetime decreases with the increase of the interlayer thickness.

The fluorescence lifetime of Au NP@SiO_2@DTA-Eu NPs with different interlayer thickness was fitted by the single exponential decay equation (Equation 1),

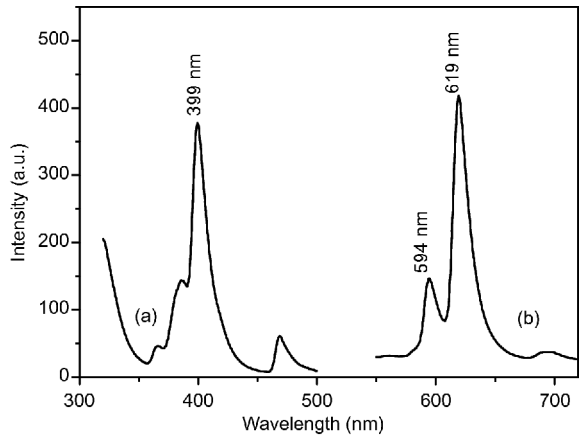

Figure 5 Fluorescence excitation spectrum (a) and fluorescence emission spectrum (b) of the Au NP@SiO_2@TDA-Eu.

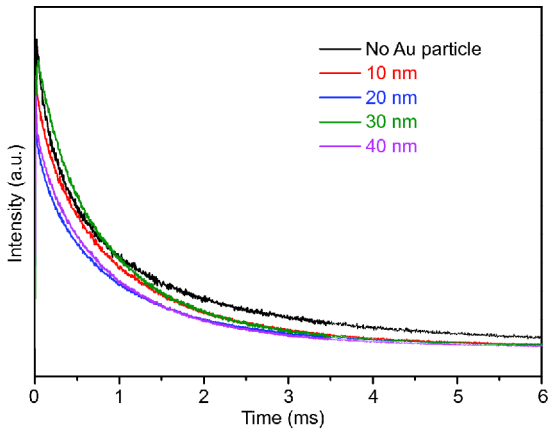

Figure 7 Decay curves of the Au NP@SiO_2@DTA-Eu nanocomposites with different silica thickness.

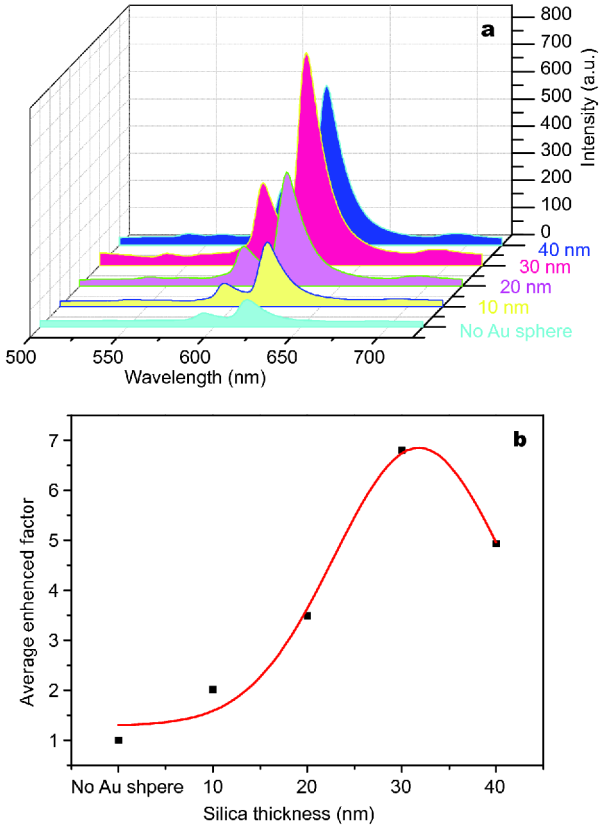

Figure 6 The Au NP@SiO_2@TDA-Eu with different thickness of silica: (a) 3D chart of emission spectra and (b) Gauss fitting curve of the average enhancement factor.

$$y = y_0 + Ae^{-(x-x_0)/t}. \quad (1)$$

The fitting curves are shown in Figs S1–S5 and fitting data are shown in Table S1.

The fluorescence lifetime of SiO_2@DTA-Eu NPs is 1.0741 ms (Fig. S1), in contrast, the average fluorescence lifetimes of Au NP@SiO_2@DTA-Eu NPs with silica thickness of 10, 20, 30 and 40 nm, are about 1.0048, 0.9909, 0.9421 and 0.9575 ms, respectively. These data indicate fluorescence decay lifetime decreases rapidly after the Au NPs are coated with silica. When the thickness of silica layer reaches 30 nm, the fluorescence lifetime decreases from 1.0741 to 0.9421 ms and the degree of decay is the strongest, which is consistent with the life decay model. It also reveals that the thickness of silica is one of the main factors of fluorescence enhancement in the nanocomposites of Au NP@SiO_2@DTA-Eu.

In order to better understand the fluorescence quenching mechanism and the detection sensitivity, DTA-Eu-H_2O_2 and Au NP@SiO_2@DTA-Eu-H_2O_2 were prepared by the reaction of DTA-Eu and Au NP@SiO_2(30 nm)@DTA-Eu with H_2O_2, respectively, for 10 min. The fluorescence quenching curves are shown in Fig. 8a, b. As expected, the emission spectra display a series of sharp lines assigned to the transitions of $^5D_0 \rightarrow {}^7F_{1\text{-}2}$. All the emissions are quenched with the increase of hydrogen peroxide; however, the fluorescence quenching of Au NP@SiO_2@DTA-Eu is stronger after adding the same amount of hydrogen peroxide. A plot of the fluorescence quenching intensity as a function of the H_2O_2 concentration gives a linear trend from 0 to 500 μmol L^{-1}. I_0 is the fluorescence intensity at the beginning without H_2O_2 and I is the fluorescence intensity after reacting with H_2O_2. DTA-Eu-H_2O_2: $y = 0.2926x - 9.3622$, $R^2 = 0.9575$, Fig. 8c; Au NP@SiO_2@DTA-Eu-H_2O_2: $y = 3.1639x + 159.28$, $R^2 = 0.9598$, Fig. 8c. Furthermore, the Au NP@SiO_2@DTA-Eu NPs are more sensitive to hydrogen peroxide solution, which is

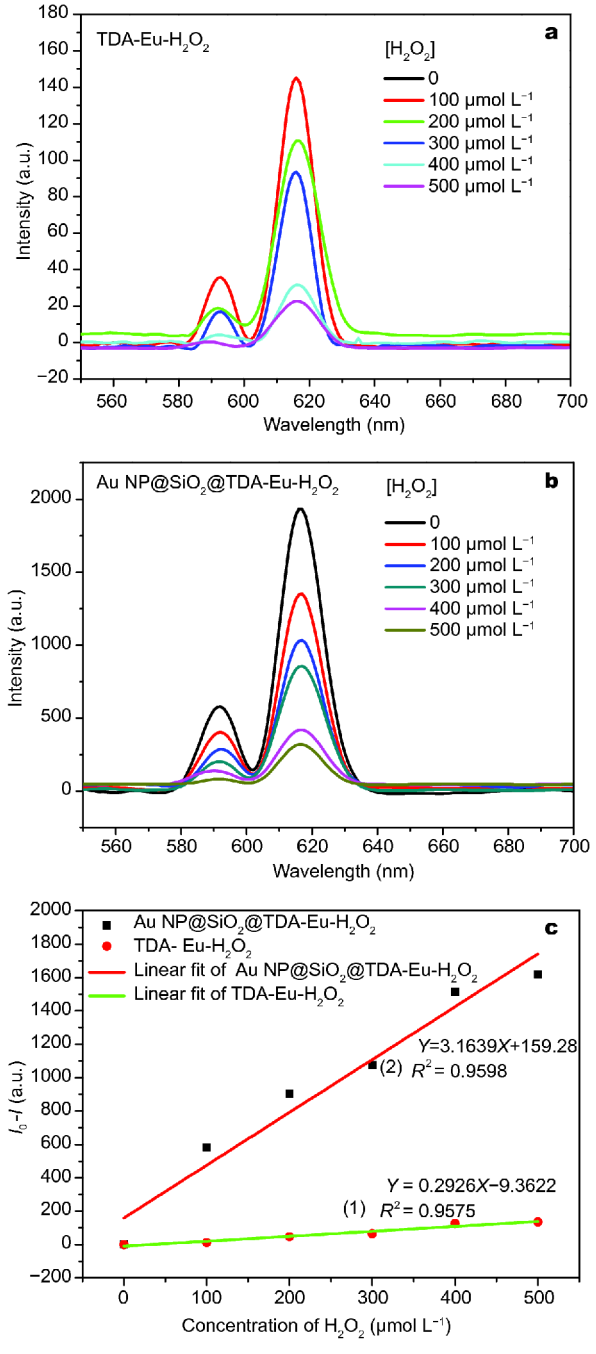

Figure 8 Fluorescence of (a) DTA-Eu-H_2O_2 and (b) Au NP@SiO_2@DTA-Eu-H_2O_2 quenched by H_2O_2 with different concentrations. (c) Plot of the fluorescence intensity (I_0-I) of $^5D_0 \rightarrow {}^7F_2$ as a function of the concentration of H_2O_2 (0–500 μmol L^{-1}, 500 μL).

due to that the S=O groups donate p-electrons to the Eu^{3+}, and it is considered that this electron-transfer process leads to the change of Eu^{3+} coordination environment and further affects the fluorescence intensity of Eu^{3+}.

CONCLUSIONS

In this work, a combination of one-pot synthesis and hydrothermal treatment was employed for the formation of Au NP@silica@europium coordination polymers denoted as Au NP@SiO_2@TDA-Eu nanocomposites. The maximum enhancement factor of the nanocomposites is 6.81 when the thickness of silica between the core of Au NP and the shell of TDA-Eu is 30 nm. It is considered that the spacer thickness is the main factor influencing the fluorescencent enhancement according to the fluorescence lifetime fittings, which is consistent with the lifetime decay model. The Au NP@SiO_2@TDA-Eu nanocomposites can be selectively quenched by reactive oxygen species and is expected to be a highly sensitive fluorescent probe. The current research would be beneficial to reactive oxygen species sensing in biological and environmental applications.

Received 7 August 2017; accepted 20 September 2017; published online 26 October 2017

1 Fuller SJ, Wragg FPH, Nutter J, *et al.* Comparison of on-line and off-line methods to quantify reactive oxygen species (ROS) in atmospheric aerosols. Atmos Environ, 2014, 92: 97–103
2 Sameenoi Y, Koehler K, Shapiro J, *et al.* Microfluidic electrochemical sensor for on-line monitoring of aerosol oxidative activity. J Am Chem Soc, 2012, 134: 10562–10568
3 Meyer LV, Schönfeld F, Müller-Buschbaum K. Lanthanide based tuning of luminescence in MOFs and dense frameworks–from mono- and multimetal systems to sensors and films. Chem Commun, 2014, 50: 8093–8108
4 Wang X, Chang H, Xie J, *et al.* Recent developments in lanthanide-based luminescent probes. Coord Chem Rev, 2014, 273-274: 201–212
5 Syamchand SS, Sony G. Europium enabled luminescent nanoparticles for biomedical applications. J Lumin, 2015, 165: 190–215
6 Wang D, Wang R, Liu L, *et al.* Down-shifting luminescence of water soluble $NaYF_4$:Eu^{3+}@Ag core-shell nanocrystals for fluorescence turn-on detection of glucose. Sci China Mater, 2017, 60: 68–74
7 Bhunia A, Gotthardt MA, Yadav M, *et al.* Salen-based coordination polymers of manganese and the rare-earth elements: synthesis and catalytic aerobic epoxidation of olefins. Chem Eur J, 2013, 19: 1986–1995
8 Müller-Buschbaum K, Beuerle F, Feldmann C. MOF based luminescence tuning and chemical/physical sensing. Microporous Mesoporous Mater, 2015, 216: 171–199
9 Decadt R, Van Hecke K, Depla D, *et al.* Synthesis, crystal structures, and luminescence properties of carboxylate based rare-earth coordination polymers. Inorg Chem, 2012, 51: 11623–11634
10 Le Natur F, Calvez G, Daiguebonne C, *et al.* Coordination polymers based on heterohexanuclear rare earth complexes: toward independent luminescence brightness and color tuning. Inorg Chem, 2013, 52: 6720–6730

11 Hasegawa Y, Nakanishi T. Luminescent lanthanide coordination polymers for photonic applications. RSC Adv, 2015, 5: 338–353
12 Janković V, Yang YM, You J, *et al.* Active layer-incorporated, spectrally tuned Au/SiO_2 core/shell nanorod-based light trapping for organic photovoltaics. ACS Nano, 2013, 7: 3815–3822
13 Chu Z, Yin C, Zhang S, *et al.* Surface plasmon enhanced drug efficacy using core–shell Au@SiO_2 nanoparticle carrier. Nanoscale, 2013, 5: 3406–3411
14 Zhang Y, Jiang H, Wang X. Cytidine-stabilized gold nanocluster as a fluorescence turn-on and turn-off probe for dual functional detection of Ag^+ and Hg^{2+}. Anal Chem Acta, 2015, 870: 1–7
15 Acuna GP, Bucher M, Stein IH, *et al.* Distance dependence of single-fluorophore quenching by gold nanoparticles studied on DNA origami. ACS Nano, 2012, 6: 3189–3195
16 Abadeer NS, Brennan MR, Wilson WL, *et al.* Distance and plasmon wavelength dependent fluorescence of molecules bound to silica-coated gold nanorods. ACS Nano, 2014, 8: 8392–8406
17 Feng AL, You ML, Tian L, *et al.* Distance-dependent plasmon-enhanced fluorescence of upconversion nanoparticles using polyelectrolyte multilayers as tunable spacers. Sci Rep, 2015, 5: 7779
18 Li M, Cushing SK, Wu N. Plasmon-enhanced optical sensors: a review. Analyst, 2015, 140: 386–406
19 Sun Y, Guo GZ, Liu Y, *et al.* Effects of noble metal nanoparticles on the luminescent properties of europium complex. Curr Nanosci, 2010, 6: 103–109
20 Ming T, Chen H, Jiang R, *et al.* Plasmon-controlled fluorescence: beyond the intensity enhancement. J Phys Chem Lett, 2012, 3: 191–202
21 Chen J, Zhang R, Han L, *et al.* One-pot synthesis of thermally stable gold@mesoporous silica core-shell nanospheres with catalytic activity. Nano Res, 2013, 6: 871–879
22 Li H, Kang J, Yang J, *et al.* Distance dependence of fluorescence enhancement in Au nanoparticle@mesoporous silica@europium complex. J Phys Chem C, 2016, 120: 16907–16912
23 Wang HS, Bao WJ, Ren SB, *et al.* Fluorescent sulfur-tagged europium(III) coordination polymers for monitoring reactive oxygen species. Anal Chem, 2015, 87: 6828–6833
24 Li Z, Wang L, Wang Z, *et al.* Modification of $NaYF_4$:Yb,Er@SiO_2 nanoparticles with gold nanocrystals for tunable green-to-red upconversion emissions. J Phys Chem C, 2011, 115: 3291–3296
25 Liz-Marzán LM, Giersig M, Mulvaney P. Synthesis of nanosized gold–silica core–shell particles. Langmuir, 1996, 12: 4329–4335
26 http://refractiveindex.info/
27 Zhang J, Fu Y, Lakowicz JR. Luminescent silica core/silver shell encapsulated with Eu(III) complex. J Phys Chem C, 2009, 113: 19404–19410
28 Saboktakin M, Ye X, Oh SJ, *et al.* Metal-enhanced upconversion luminescence tunable through metal nanoparticle–nanophosphor separation. ACS Nano, 2012, 6: 8758–8766
29 Deng W, Jin D, Drozdowicz-Tomsia K, *et al.* Ultrabright Eu-doped plasmonic Ag@SiO_2 nanostructures: time-gated bioprobes with single particle sensitivity and negligible background. Adv Mater, 2011, 23: 4649–4654
30 Lakowicz JR. Radiative decay engineering 5: metal-enhanced fluorescence and plasmon emission. Anal Biochem, 2005, 337: 171–194
31 Park W, Lu D, Ahn S. Plasmon enhancement of luminescence upconversion. Chem Soc Rev, 2015, 44: 2940–2962
32 Gryczynski I, Malicka J, Gryczynski Z, *et al.* Radiative decay engineering 4. Experimental studies of surface plasmon-coupled directional emission. Anal Biochem, 2004, 324: 170–182
33 Zhang H, Li Y, Ivanov IA, *et al.* Plasmonic modulation of the upconversion fluorescence in $NaYF_4$:Yb/Tm hexaplate nanocrystals using gold nanoparticles or nanoshells. Angew Chem, 2010, 122: 2927–2930

Acknowledgements This work was financially supported by the National Natural Science Foundation of China (51702006 and 21501141), the Doctoral research project (ZK2017027) of Baoji University of Arts and Sciences, and the Education Commission of Shaanxi Province (2015JQ6223, 12JS114, 14JS092 and 17JS009).

Author contributions Li H and Yang J proposed the research and guided the project. Deng Q, Dou S and Zhao W designed and performed the experiments. Lin C and Liu X analyzed and discussed the experimental results, Li H and Deng Q drafted the manuscript. All the authors checked and approved the manuscript.

Conflict of interest The authors declare that they have no conflict of interest.

Supplementary information Supporting data are available in the online version of the paper.

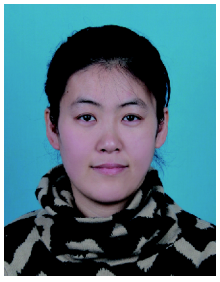

Huiqin Li received her BSc degree from Shaanxi University of Science and Technology and PhD degree from Northwestern University. Now, she is a lecturer at Baoji University of Arts and Sciences. Her research interest focuses on the functional nanomaterials and luminescent materials.

Jianhui Yang received PhD degree from Changchun Institute of Applied Chemistry, Chinese Academy of Sciences in 2008. Then, he had his post-doc experience from the City University of New York, University of Florida, the University of Texas at San Antonio and the University of Paris. Currently, he is an associate professor at Northwestern University. His research interests include controllable synthesis, assembly and properties of nanomaterials.

复合纳米材料Au@SiO_2@Eu配位聚合物的荧光增强及其对活性氧的高灵敏检测研究

李慧勤[1*], 杨建辉[2*], 邓青青[2], 窦树梅[1], 赵微微[1], 林冲[2], 刘晓芳[2]

摘要 本论文通过两步工艺成功合成了Au NP@SiO_2@TDA-Eu复合纳米材料: 采用改进的一锅法制备了纳米复合材料Au NP@SiO_2, 然后利用水热法, 在无水乙醇中通过亚硫基二乙酸[$S(CH_2COO)_2^{2-}$, TDA]和$Eu(NO_3)_3{\cdot}6H_2O$反应, 生成铕的配位聚合物, 并将其沉积在Au NP@SiO_2的表面合成复合纳米材料Au NP@SiO_2@TDA-Eu. 该复合材料在二氧化硅层厚度为30 nm时, 荧光增强最大, 增强因子为6.81, 在对活性氧的检测中, 表现出高灵敏度.

